



**HAL**  
open science

## How the insula speaks to the heart: Cardiac responses to insular stimulation in humans

Florian Chouchou, François Mauguière, Ophélie Vallayer, Hélène Catenox, Jean Isnard, Alexandra Montavont, Julien Jung, Vincent Pichot, Sylvain Rheims, Laure Mazzola

### ► To cite this version:

Florian Chouchou, François Mauguière, Ophélie Vallayer, Hélène Catenox, Jean Isnard, et al.. How the insula speaks to the heart: Cardiac responses to insular stimulation in humans. *Human Brain Mapping*, 2019, 40 (9), pp.2611-2622. 10.1002/hbm.24548 . hal-03962741

**HAL Id: hal-03962741**

**<https://hal.science/hal-03962741>**


Submitted on 30 Jan 2023

**HAL** is a multi-disciplinary open access archive for the deposit and dissemination of scientific research documents, whether they are published or not. The documents may come from teaching and research institutions in France or abroad, or from public or private research centers.

L'archive ouverte pluridisciplinaire **HAL**, est destinée au dépôt et à la diffusion de documents scientifiques de niveau recherche, publiés ou non, émanant des établissements d'enseignement et de recherche français ou étrangers, des laboratoires publics ou privés.

## RESEARCH ARTICLE

# How the insula speaks to the heart: Cardiac responses to insular stimulation in humans

Florian Chouchou<sup>1</sup>  | François Mauguière<sup>2,3</sup> | Ophélie Vallayer<sup>4</sup> | Hélène Catenoux<sup>2,5</sup> | Jean Isnard<sup>2,3</sup> | Alexandra Montavont<sup>2,5</sup> | Julien Jung<sup>2,5</sup> | Vincent Pichot<sup>6</sup> | Sylvain Rheims<sup>2,5</sup> | Laure Mazzola<sup>3,4</sup>

<sup>1</sup>IRISSE Laboratory (EA4075), UFR SHE, University of La Réunion, Le Tampon, France

<sup>2</sup>Department of Functional Neurology and Epileptology, Hospices Civils de Lyon, Université de Lyon, Lyon, France

<sup>3</sup>NeuroPain Lab, Lyon Neuroscience Research Centre, CRNL – INSERM U 1028/CNRS UMR 5292, University of Lyon, Lyon, France

<sup>4</sup>Neurology Department, University Hospital, Saint-Etienne, France

<sup>5</sup>TIGER Lab, Lyon Neuroscience Research Centre, CRNL – INSERM U 1028/CNRS UMR 5292, University of Lyon, Lyon, France

<sup>6</sup>EA SNA-EPIS 4607, Department of Clinical and Exercise Physiology, University of Lyon, Jean Monnet University, Saint-Etienne, France

## Correspondence

Florian Chouchou, IRISSE Laboratory (EA4075), UFR SHE, University of La Réunion, 117 rue du General Ailleret, 97430 Le Tampon, France.

Email: florianchouchou@gmail.com

## Abstract

Despite numerous studies suggesting the role of insular cortex in the control of autonomic activity, the exact location of cardiac motor regions remains controversial. We provide here a functional mapping of autonomic cardiac responses to intracortical stimulations of the human insula. The cardiac effects of 100 insular electrical stimulations into 47 epileptic patients were divided into tachycardia, bradycardia, and no cardiac response according to the magnitude of RR interval (RRI) reactivity. Sympathetic (low frequency, LF, and low to high frequency powers ratio, LF/HF ratio) and parasympathetic (high frequency power, HF) reactivity were studied using RRI analysis. Bradycardia was induced by 26 stimulations (26%) and tachycardia by 21 stimulations (21%). Right and left insular stimulations induced as often a bradycardia as a tachycardia. Tachycardia was accompanied by an increase in LF/HF ratio, suggesting an increase in sympathetic tone; while bradycardia seemed accompanied by an increase of parasympathetic tone reflected by an increase in HF. There was some left/right asymmetry in insular subregions where increased or decreased heart rates were produced after stimulation. However, spatial distribution of tachycardia responses predominated in the posterior insula, whereas bradycardia sites were more anterior in the median part of the insula. These findings seemed to indicate a posterior predominance of sympathetic control in the insula, whichever the side; whereas the parasympathetic control seemed more anterior. Dysfunction of these regions should be considered when modifications of cardiac activity occur during epileptic seizures and in cardiovascular diseases.

## KEYWORDS

autonomic nervous system, bradycardia, heart, insula, RR intervals, tachycardia

## 1 | INTRODUCTION

The autonomic nervous system (ANS) is crucial for many aspects of our daily life. Its regulatory action on cardiovascular, respiratory, digestive, endocrine, and many other systems allows the body to respond to the metabolic demands of motor, emotional, and cognitive challenges (Critchley, 2005; Smith, Thayer, Khalsa, & Lane, 2017). Some of the most important integrative control centers for ANS functions are located in the brainstem (Guyenet, 2006). However, growing evidence supports that cortical regions are involved in autonomic

control (Beissner, Meissner, Bär, & Napadow, 2013; Ruiz Vargas, Sörös, Shoemaker, & Hachinski, 2016). The core elements of this central autonomic network consist of the amygdala, anterior cingulate, ventromedial prefrontal cortex, inferior and medial frontal gyrus, and anterior and posterior insula (Beissner et al., 2013; Benarroch, 1993; Cechetto, 2014; Critchley & Harrison, 2013; Lacuey et al., 2017; Ruiz Vargas et al., 2016; Verberne & Owens, 1998).

The role played by the insula in the control of the autonomic system and regulation of cardiac function, recently reviewed by Oppenheimer and Cechetto (2016), is supported by stimulation experiments

mostly in rats (Hoffman & Rasmussen, 1953; Oppenheimer & Cechetto, 1990) but also by data in humans based on stimulation (Oppenheimer, Gelb, Girvin, & Hachinski, 1992), lesion (Sörös & Hachinski, 2012; Tokgözüoglu et al., 1999), and neuroimaging studies (Beissner et al., 2013; Ruiz Vargas et al., 2016). However, the location of insular subregions involved in this control shows large variations across studies, particularly along the rostro-caudal axis. Similarly, the lateralization of cardiac regulation in the right insula for sympathetic control and in the left insula for parasympathetic control reported by some authors (Lacuey et al., 2017; Oppenheimer et al., 1992; Oppenheimer & Cechetto, 2016; Ruiz Vargas et al., 2016) was not confirmed by others (Chouchou et al., 2017; Marins et al., 2016; Szurhaj et al., 2015).

So despite these numerous studies suggesting the role of insular cortex in the control of autonomic activity, the exact location of cardiac motor regions in the insula and their potential lateralization remain controversial. Moreover, neuroimaging studies used cardiac activation paradigms, raising the question whether the observed activations of the insular cortex reflect a control on heart activity or the processing of information coming from the heart itself. Direct electrical stimulation of the insular cortex in awake patients implanted with depth electrodes bypasses this difficulty and offers a unique opportunity to address this issue. Measurement of heart rate variability using electrocardiographic (EKG) RR interval (RRI) has become an increasingly used noninvasive tool for examining sympathetic and parasympathetic activities and is well suited to probe the influence of the ANS on heart activity. The power of high frequency (HF) variations of the RRI proved to be a reliable marker of parasympathetic control of cardiac rhythm, while that of the low frequency (LF) RRI variations and the ratio of low to high frequency powers (LF/HF ratio) are markers of the sympathovagal balance (Chouchou & Desseilles, 2014; Malliani, Pagani, Lombardi, & Cerutti, 1991; Pagani et al., 1997; Pichot, Roche, Celle, Barthélémy, & Chouchou, 2016). If the HF is exclusively modulated by parasympathetic activity, LF is under the control of both the sympathetic and parasympathetic systems (Malliani et al., 1991), so that the LF/HF ratio is proposed as a marker of sympathovagal balance, helping the assessment of sympathetic activity, even if not specific.

In this study we provide a functional mapping of autonomic cardiac responses to electrical stimulations of the human insula using a time-frequency analysis of RR variations (Pichot et al., 1999; Pichot et al., 2016) for assessing the influence of these stimulations on the sympathetic and parasympathetic controls of cardiac activity.

## 2 | PATIENTS & METHODS

### 2.1 | Patients

The 47 patients (27 women, mean age  $30.0 \pm 10.1$  (mean  $\pm$  standard deviation [SD]) years) included in this study underwent a stereoelectroencephalography (SEEG) exploration of the perisylvian and insular cortex in our Epilepsy Department at the Neurological Hospital of Lyon, between March 1997 and December 2016, with the purpose of localizing their epileptogenic area before surgery. The choice of

SEEG targets was based on video EEG recordings of seizures, interictal fluorodeoxyglucose positron emission tomography, interictal and ictal single photon emission computed tomography, and 1.5 Tesla brain magnetic resonance imaging (MRI) data. Patients with a MRI lesion in the insula and those with a seizure onset zone or a rapid propagation of ictal discharges in the insula were excluded from this study. None of the patients had known arrhythmia, cardiac pathology or took medication that could affect the ANS.

Electrical stimulation of the cortex is a routine procedure to evaluate the epileptic threshold and to provide a functional map in the explored areas. In agreement with French regulations relative to invasive investigations with a direct individual benefit, patients were fully informed about electrode implantation, stereotactic EEG and cortical stimulation procedures used to localize the epileptogenic and functionally eloquent cortical areas. All patients were fully informed of the purpose and risks of the SEEG procedure and gave their written consent. The local ethics committee approved this study.

### 2.2 | Electrodes stereotactic implantation and insular sites location

The stereotactic implantation followed the procedure described in our previous studies (Mazzola et al., 2014; Mazzola et al., 2017; Mazzola, Isnard, & Mauguière, 2006). Electrodes were implanted perpendicular to the midsagittal plane and were left in place chronically up to 15 days. The electrodes had a diameter of 0.8 mm and contained from 5 to 15 recording contacts. Contacts were 2 mm long and separated by 1.5 mm from one another. A cerebral angiogram was performed in stereotactic conditions using an X-ray source 4.85 m away from the patient's head to eliminate the linear enlargement due to X-ray divergence. The stereotactic coordinates of each electrode were calculated preoperatively on the individual cerebral MRI previously enlarged at scale 1. Cerebral MRI and angiographic images were superimposed to avoid any risk of vascular injury during implantation.

From 1997 to 2008 a postimplantation frontal X-ray at scale 1 was performed at the end of the surgery and superimposed on individual T1-weighted brain MRI to check for the final position of each electrode with respect to the targeted anatomical structures and to individualize contacts located in the insula. Since 2009, MRI-compatible electrodes have been used to confirm on individual brain MRI the position of contacts in the insular cortex.

All the 100 insular stimulation sites were localized using Talairach space with x, y, and z coordinates for mediolateral, rostrocaudal, and vertical axes, respectively. In this stereotactic space,  $x = 0$  was the coordinate of the sagittal interhemispheric plane,  $y = 0$  was that of the frontal plane passing through the vertical anterior commissure, and  $z = 0$  was that of the horizontal plane passing through the anterior and posterior commissure (AC-PC plane). AC-PC distance was normalized for each patient. The stereotactic coordinates of each stimulation site were those of the point located halfway between the two adjacent contacts used for bipolar stimulation (i.e., the center of the sphere of neural elements activated by electrical stimulation). We chose to analyze localization of stimulated contacts using Talairach coordinates in order to have a no preconception approach. Using anatomical subregions would have consisted in a region of interest

analysis, whereas several works have shown that insula anatomical subregions do not necessarily match with functional or cytoarchitectonic insula organization (Kurth, Zilles, Fox, Laird, & Eickhoff, 2010).

## 2.3 | Recording procedures

### 2.3.1 | Stimulations

Electrical stimulations were produced by a current-regulated neurostimulator designed for a safe diagnostic stimulation of the human brain, according to the routine procedure used in the department to map functionally eloquent and epileptogenic areas (Mazzola et al., 2006; Mazzola et al., 2014; Mazzola, Royet, et al., 2017). Bipolar stimulations were performed in contacts located in the gray matter. Stimulations were applied at 50 Hz, with pulse duration of 0.5 ms, train duration of 3 or 5 s, and intensity between 0.2–3.5 mA. This stimulation paradigm, along with the bipolar mode of stimulation using adjacent contacts, ensured a good spatial specificity of stimulation of within 5.5 mm around the stimulated dipole (Nathan, Sinha, Gordon, Lesser, & Thakor, 1993). Stimulus intensity was raised from 0.2 mA by steps of 0.4 mA until any sensation was obtained, and to a maximum of 3.5 mA. The stimulation threshold was defined as the minimal intensity necessary to evoke any clinical response. No stimulation was delivered at suprathreshold values. During the stimulation session, patients were sitting in bed and asked to relax. Subjective reports and clinical observations evoked by each stimulation were collected immediately. EEG data and videos were analyzed retrospectively to characterize clinical evoked sensations.

### 2.3.2 | SEEG recordings

Online SEEG recordings (Micromed BrainQuick®, Lyon, France) were obtained using a 128-channel amplified device at a sampling frequency of 256 Hz and a band-pass filter of 0.03–100 Hz. The reference electrode was chosen for each patient on an implanted contact located in the skull. SEEG was recorded continuously and was stored for offline analysis. All SEEG signals were referenced using bipolar montages between neighboring contacts of the same electrode. SEEG data were also retrospectively analyzed to eliminate from analysis sites where stimulation triggered an after discharge and those where abnormal rhythms (such as rapid rhythms or continuous spike activity) suggesting a cortical focal dysplasia undetectable on MRI were recorded.

### 2.3.3 | ECG recordings

Two to three electrodes placed on the thorax were dedicated to ECG acquisition. For each patient, we selected the electrode with the highest signal-to-noise amplitude for offline analysis. The acquisition of ECG signal was done with the same parameters as SEEG, at a sampling frequency of 256 Hz and a band-pass filter of 0.03–100 Hz. ECG was recorded continuously and data were stored for offline analysis.

## 2.4 | Data analyses

### 2.4.1 | Autonomic cardiac reactivity analysis

EKG signals were subjected to peak-to-peak analysis to detect QRS complex (R waves) to calculate the RRI signal using dedicated software (Pichot et al., 2016). Initial automatized extraction of RRI signal

from ECG data was subsequently checked by visual inspection; so in the presence of undetected isolated QRS, ectopic beats or artifacts, the RRI signal was manually corrected. If correction was not possible, a cubic spline interpolation was used to correct for isolated artifacts and ectopic beats (Daskalov & Christov, 1997; Pichot et al., 2016). EKG data were eliminated from analysis when uncorrected artifacts or ectopic beats occurred in an interval of less than 15 heartbeats before and 25 heartbeats after the electrical stimulus.

### 2.4.2 | RRIs analysis

In order to estimate autonomic cardiac modifications over time, a wavelet analysis was applied to the RRI signal. This time-frequency analysis was used because wavelet transform allows analysis of non-stationary signals and provides temporally localized information; its ability to study autonomic reactivity had been validated by dual atropine and propranolol blockade (Pichot et al., 1999; Rajendra Acharya, Paul Joseph, Kannathal, Lim, & Suri, 2006). Wavelet transform was used to decompose the RR signal in time and frequency domains (Chouchou et al., 2011; Pichot et al., 2016) using the mother function Daubechies four. Wavelet analysis was applied to a 2.4 Hz resampled RRI signal. Fast frequencies in RR signals were gathered in HF ( $ms^{-2}$ , 0.15–0.4 Hz) to assess parasympathetic reactivity, and in LF ( $ms^{-2}$ , 0.04–0.15 Hz) to assess sympathetic reactivity. As LF is controlled by both the sympathetic and parasympathetic systems, while HF is only controlled by the parasympathetic system, the LF/HF ratio was used to assess sympathovagal balance (Malliani et al., 1991; Pagani et al., 1997).

### 2.4.3 | Categories of autonomic cardiac responses evoked by electrical stimulations

For each electrical stimulation, after visual inspection of our data, evoked cardiac responses were divided into three groups (i.e., tachycardia, bradycardia, and no cardiac response) following the three steps that we already adopted to study ictal tachycardia in temporal lobe seizures (Chouchou et al., 2017): (a) RRI values were normalized in percentage of the basal period values (mean of 10 prestimulation heartbeats) to eliminate interindividual variability. (b) The baseline mean and *SD* of RRIs were calculated over a prestimulation period of 10 heartbeats. (c) The mean RRI of the five poststimulation heart beats was used for detection of RRI changes: tachycardia was defined as a RRI decrease below the baseline mean  $- 1 SD$ , and bradycardia as a RRI increase over the baseline mean  $+ 1 SD$ . Poststimulation mean RRI in the interval baseline mean  $\pm 1 SD$  were considered as no cardiac response. As the RRI signal is very volatile, the categorization of responses was based on five poststimulation heartbeats to detect immediate cardiac responses to stimulation and to avoid consideration of cardiac changes unrelated to stimulation.

## 2.5 | Statistical analyses

For all statistical analyses, we used Statview® software (SAS Institute, Inc., Cary, NC). For each variable of interest, normality of distribution was tested using Kolmogorov–Smirnov test for normality.

The mean RRIs of 10 heartbeats pre-stimulus and 5 heartbeats post-stimulus were submitted to a two-sided repeated-measures

analysis of variance (ANOVA) with one within factor *time* (before and after electrical stimulation) and two between factors: cardiac response (tachycardia, bradycardia, and no cardiac response) and lateralization of stimulations (left and right). Latencies of the maximum of RRI changes for bradycardia and tachycardia in the post-stimulation period (between the first and tenth heartbeat after stimulation) were studied using an ANOVA with one between factor (tachycardia vs. bradycardia).

We used a time analysis of 10 heartbeats pre- and post-stimulus for statistical analysis of these parameters because the changes of HF, LF, and LF/HF ratio can be slower than RRI variations. Mean of HF, LF, and LF/HF ratio corresponding to 10 heartbeats were therefore submitted to a two-sided repeated-measures ANOVA with the same within factor time and two between factors: cardiac response and lateralization of stimulations.

As stimulated contacts with a negative  $\times$  coordinate are located in the left hemisphere and those with a positive  $\times$  coordinate in the right one, we used the absolute value of  $\times$  coordinate for statistical analysis but introduced lateralization as a factor.

Talairach coordinates were submitted to a two-sided ANOVA with two between factors: the cardiac response (tachycardia, bradycardia, and no cardiac response) and the lateralization of stimulations (left and right).

The relationship between clinical sensation evoked by stimulation and cardiac responses (tachycardia, bradycardia, and no cardiac response) was analyzed using two-sided Pearson's two-sided  $\chi^2$  test.

To control for potential confounding factors, we also submitted intensities of stimulation, inter-stimulation intervals, and age of patients to a two-sided ANOVA with two between factors: the cardiac response (tachycardia, bradycardia, and no cardiac response) and the lateralization of stimulations (left and right). Sex ratio was also compared using two-sided Pearson's two-sided  $\chi^2$  test according to the cardiac response and the lateralization of stimulations.

Student–Newman–Keuls post hoc test for multicomparisons was performed when appropriate. *p*-values were considered as significant at  $p < 0.05$ .

## 3 | RESULTS

### 3.1 | Type of evoked cardiac responses

A total of 100 electrical stimulations of the insular cortex were studied (51 on the left side and 49 on the right side). The mean number of stimulation per patient was  $2.09 \pm 1.60$  (range: 1–9). Forty-seven stimulations (47%) produced a cardiac response. The rates of cardiac responses were not different between right (19%) and left (28%) stimulations ( $df = 1$ ,  $\chi^2 = 2.00$ ,  $p = 0.157$ ). Bradycardia was induced by 26 stimulations (26%) and tachycardia by 21 stimulations (21%). No significant lateralization of the type of cardiac response was observed, as right and left insula stimulations induced bradycardia as often as tachycardia (left stimulations: bradycardia: 33%, tachycardia 18%; right stimulations: bradycardia: 22%, tachycardia 20%;  $df = 2$ ,  $\chi^2 = 3.40$ ,  $p = 0.183$ ).

### 3.2 | Time course of cardiac reactivity to insular stimulation

RRI varied significantly between pre- and post-stimuli periods for both tachycardia and bradycardia: the RRI decreased in tachycardia ( $p < 0.05$ ) and increased in bradycardia ( $p < 0.05$ ). No differences in RRI variations were found between right and left insular stimulations.

Statistical analysis of the cardiac reactivity revealed differences in the RRI variations time course according to the type of cardiac evoked responses. Table 1a summarizes the results of ANOVAs. Figure 1a illustrates the time course of RRI variations (mean and SD) for each type of evoked cardiac response (bradycardia [ $n = 26$ ], tachycardia [ $n = 21$ ] and no cardiac response [ $n = 53$ ]). Cardiac responses were present from the onset of stimulation. The maximum of RRI changes happened earlier for bradycardia ( $2.9 \pm 1.6$  heartbeats) than for tachycardia ( $5.9 \pm 2.4$  heartbeats) after stimulation ( $p < 0.001$ ).

### 3.3 | Relationship between cardiac responses and clinically evoked sensations

Ten of the 100 insular stimulations (10%) did not produce any clinical sensation. The other 90 stimulations evoked clinical responses that consisted in somatosensitive sensations (paresthesiae, thermal, or pain) in 50% ( $n = 50$ ), visceral sensation (constrictive sensation in abdomen or throat, nausea, facial blush, etc.) in 37% ( $n = 37$ ) and other type of sensation (auditory, vertigo, taste, odor, etc.) in 12% ( $n = 12$ ). No patient reported a subjective sensation of heart rate modification. Most of stimulations produced a single type of clinical sensation ( $n = 81$ ), but some could produce a combination of sensations (for example paresthesiae in the face and nasty taste) ( $n = 9$ ). No relationship was found between the type of cardiac responses and evocation of somatosensitive sensations, visceral sensations, other type of sensations, or the absence of clinical response ( $df = 8$ ,  $\chi^2 = 3.68$ ,  $p = 0.884$ ).

### 3.4 | Parameters of intracortical stimulations and demographic data

The electrical stimulations were performed during sessions in which several cortical sites were stimulated. So to ensure that these stimulation conditions or differences between patients did not influence the autonomic cardiac responses, we assessed the stimulation intensity, the time interval between stimulations, the age, as well as the gender of the patients (Table 1c,d). We observed that the mean stimulation intensity was  $1.6 \pm 1.0$  mA, without significant difference between right and left stimulations ( $F[1,99] = 1.78$ ,  $p = 0.185$ ) and that stimulation intensity had no effect on the type of cardiac response ( $F[2,99] = 1.02$ ,  $p = 0.364$ ). Time intervals between the studied stimulation and the preceding and following stimulations were of  $138.5 \pm 95.3$  s and  $143.5 \pm 83.4$  s, respectively, and were thus long enough to avoid an overlap between cardiac responses. Moreover, there was no significant difference in inter-stimulation intervals between right and left stimulations ( $p = 0.326$  and  $p = 0.108$ , before and after stimulation, respectively). Lastly, there was no effect of age ( $p = 0.714$ ) or of sex ( $p = 0.590$ ) on the type of cardiac responses.



**TABLE 1** Results of analysis of variance for (a) autonomic and cardiac parameters, (b) Talairach coordinates, (c) demographic data, and (d) parameters of intracortical stimulations

	Time		Cardiac response		Lateralization		Interaction lateralization - cardiac response		Interaction time - cardiac response		Interaction time - lateralization		Overall interaction	
	F	p	F	p	F	p	F	p	F	p	F	p	F	p
	<b>A—autonomic and cardiac parameters</b>													
RRI (ms)	7.95	0.006	34.31	< 0.001	0.45	0.504	0.47	0.626	26.19	< 0.001	0.17	0.680	0.11	0.898
LF (ms <sup>2</sup> )	2.39	0.127	0.04	0.959	1.66	0.202	2.39	0.127	0.04	0.959	1.66	0.202	0.75	0.477
HF (ms <sup>2</sup> )	6.81	0.011	4.09	0.021	1.30	0.259	0.86	0.429	4.09	0.021	1.30	0.259	0.86	0.429
LF/HF	5.87	0.018	3.25	0.045	0.92	0.402	0.92	0.402	3.25	0.045	5.87	0.018	0.92	0.402
<b>B—coordinates</b>														
Y			4.57	0.013	0.01	0.917	1.94	0.145						
Z			0.67	0.514	0.12	0.735	3.86	0.024						
<b>C—demographic data</b>														
Age			0.34	0.714	1.07	0.347	2.63	0.080						
<b>D—parameters of intracortical stimulations</b>														
Intensity stimulation			1.51	0.227	3.01	0.086	0.31	0.733						
Inter-stimulation intervals before stimulations			0.62	0.547	2.33	0.130	1.36	0.261						
Inter-stimulation intervals after stimulations			0.07	0.931	2.64	0.108	0.46	0.632						

### 3.5 | Autonomic reactivity underlying cardiac reactivity

To better understand the autonomic changes that explain these cardiac responses, we analyzed RRI variability before and after the insula stimulation, according to the lateralization of the stimulation and the type of evoked cardiac response.

The parameters used to study cardiac parasympathetic response showed the following results (Table 1): The HF power of RRI varied significantly (Table 1a; Figure 1c) between pre- and post-stimulation periods for bradycardia ( $p < 0.05$ ). There was also a significant difference in HF power in the poststimulation period between bradycardia and tachycardia ( $p < 0.05$ ) and between bradycardia and no cardiac response ( $p < 0.05$ ).

This HF power increase during post-stimulation bradycardia indicated that this effect reflects an early increase in parasympathetic tone after the stimulation. The slight and later decrease of HF power associated with tachycardia was not significant compared to pre-stimulation baseline, indicating that this effect did not underpin the changes in the RRI time course.

The parameters used to study cardiac sympathetic response showed the following results (Table 1): LF power (Figure 1b; Table 1a) did not vary significantly between pre- and post-stimulation periods ( $p = 0.127$ ), whatever the type of evoked cardiac response ( $p = 0.959$ ) or the side of stimulation ( $p = 0.202$ ). However, the LF/HF ratio (Figure 1d) varied significantly with time ( $p = 0.018$ ) and with the type of cardiac response ( $p = 0.045$ ). Post hoc test revealed a significant increase in LF/HF ratio between pre- and post-stimulation periods in tachycardia ( $p < 0.05$ ), but also a significant difference between tachycardia and bradycardia ( $p < 0.05$ ). Considering the absence of modification of the HF between the pre- and post-stimulation periods for tachycardia, this increase in LF/HF ratio during post-stimulation

period in tachycardia may suggest that this effect reflects an increase in sympathetic tone, while there was no significant change of LF/HF ratio associated to bradycardia.

### 3.6 | Functional mapping of autonomic cardiac responses in the insula

Talairach stereotactic coordinates (mean  $\pm$  SD) of the insula contacts where electrical stimulation evoked a cardiac response are presented in Table 2 and ANOVAs in Table 1b. Figure 2a illustrates the spatial distribution of sites where stimulation evoked a cardiac response superimposed onto the distribution of sites where stimulation produced no cardiac response. Despite an overlap in the spatial distribution of the different types of cardiac responses, most of tachycardiac responses were obtained after stimulation of a relatively limited area located in the posterior-ventral part of the insula, corresponding mainly to the posterior long gyrus, with a few ectopic sites located in the upper part of the middle insula. Sites where stimulation produced bradycardia were more scattered in the insula covering an area from posterior to middle insular cortex. Figure 2b shows the barycenters and SDs of Talairach coordinates where stimulation evoked tachycardia, bradycardia, or no cardiac response. Statistical analysis revealed that coordinates of stimulated sites in the y-axis were significantly different according to the type of evoked cardiac response but not according to the hemispheric lateralization of the stimulation (Table 1b). Post hoc test showed more negative coordinates along the y-axis for tachycardia than for bradycardia and "no cardiac response" sites ( $p < 0.05$ ), suggesting that the representation of tachycardia, and hence of sympathetic control, is posterior to that of bradycardia and parasympathetic control.

For the z-axis, statistical analysis showed that coordinates of stimulated sites were not significantly different according to the type

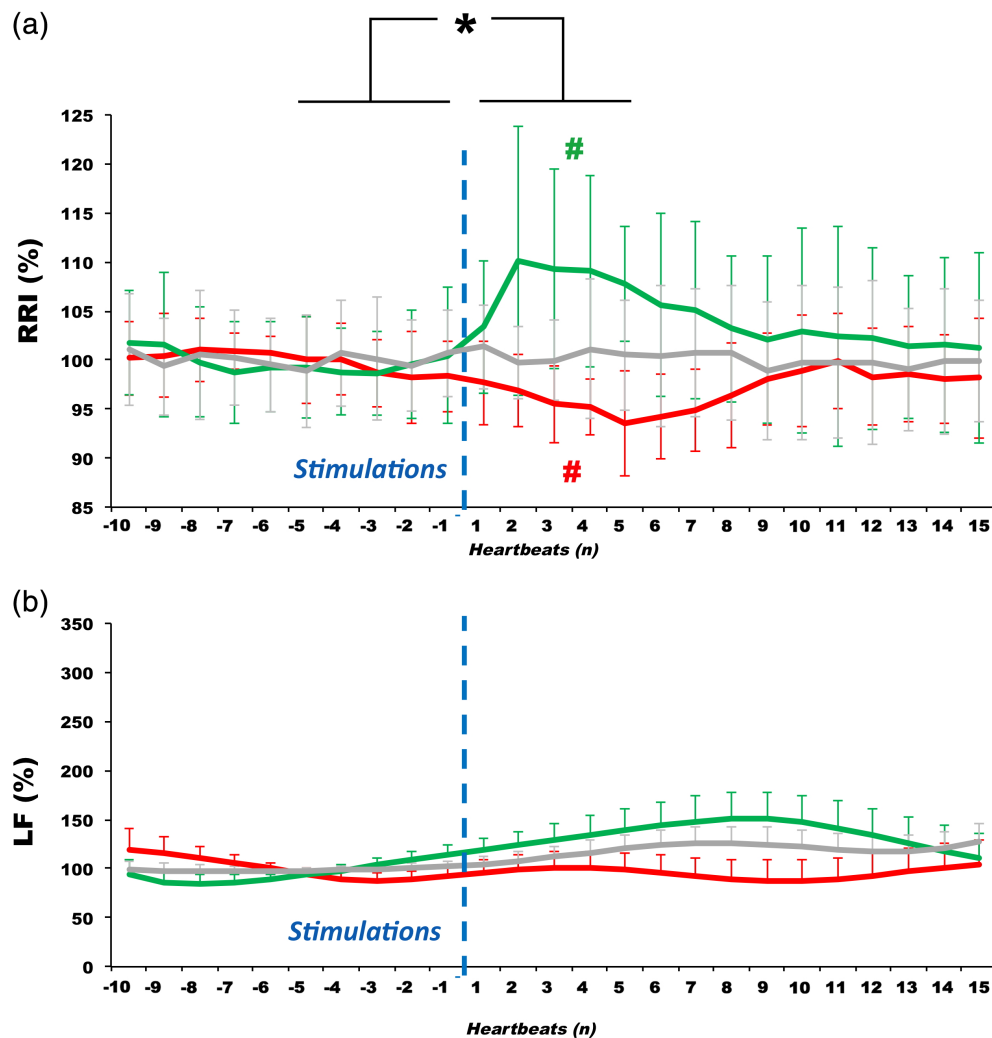


**FIGURE 1** Autonomic cardiac reactivity to insular stimulations. Time course of (a) RR intervals (RRI), (b) low frequency power (LF), (c) high frequency power (HF), and (d) LF/HF ratio variations (mean and standard deviation), before (10 heartbeats) and after (15 heartbeats) electrical stimulations in the insular cortex according to the type of evoked cardiac response (bradycardia, tachycardia, and no cardiac response). Data were normalized in percentage, relative to the basal period values. Both tachycardia and bradycardia were evoked by insular electrical stimulations, whichever the side of stimulations. Parasympathetic reactivity was underpinned by changes in HF during bradycardia, whereas sympathetic reactivity by changes in LF/HF during tachycardia. For RRI, statistical analysis was applied to the mean of five heartbeats pre- and post-stimulus, and for parameters of RRI variability on the mean of 10 heartbeats pre- and post-stimulus\* $p < 0.05$  from baseline. # $p < 0.05$  from the other two evoked cardiac responses. Vertical dotted lines symbolize stimulation onset [Color figure can be viewed at [wileyonlinelibrary.com](http://wileyonlinelibrary.com)]

of evoked cardiac response or to the lateralization of the stimulation (Table 1b). However, an interaction was significant between the lateralization and type of evoked response (Tables 1b and 2). Although no post hoc statistical effect emerged, it seemed that a general interaction effect appeared, as illustrated in Figure 3 showing that tachycardia might be preferentially evoked by stimulating the ventral posterior part of the insula on the right side, and its dorsal posteromedian part on the left side; whereas bradycardia might be mainly induced by stimulating the dorsal insula on the right side and the ventral insula on the left side.

## 4 | DISCUSSION

Our study is the first focusing on cardiac effects of direct electrical stimulations of the human insular cortex using SEEG. The main findings are as follows: (a) the major role of insula in central control of

cardiac function is confirmed because almost 50% of insular stimulations induced a modification of cardiac activity; (b) RRI changes induced by direct electrical stimulation of insula were subtle and brief; (c) tachycardiac responses were underpinned by sympathetic reactivity, and bradycardia by parasympathetic control; (d) the functional mapping of cardiac responses in the insula showed that the representation of tachycardia is more posterior than that of bradycardia; (e) cardiac response rates and types (tachycardia or bradycardia) were equally represented in right and left insula; and (f) there might be some left/right asymmetry in insular subregions where increased or decreased heart rates were produced. Although not significant, stimulation of the dorsal insula seemed to lead to more tachycardiac responses on the left side and to more bradycardiac responses on the right side. Conversely, stimulation of the ventral insula seemed to lead to more bradycardiac responses on the left side and to more tachycardiac responses on the right side.

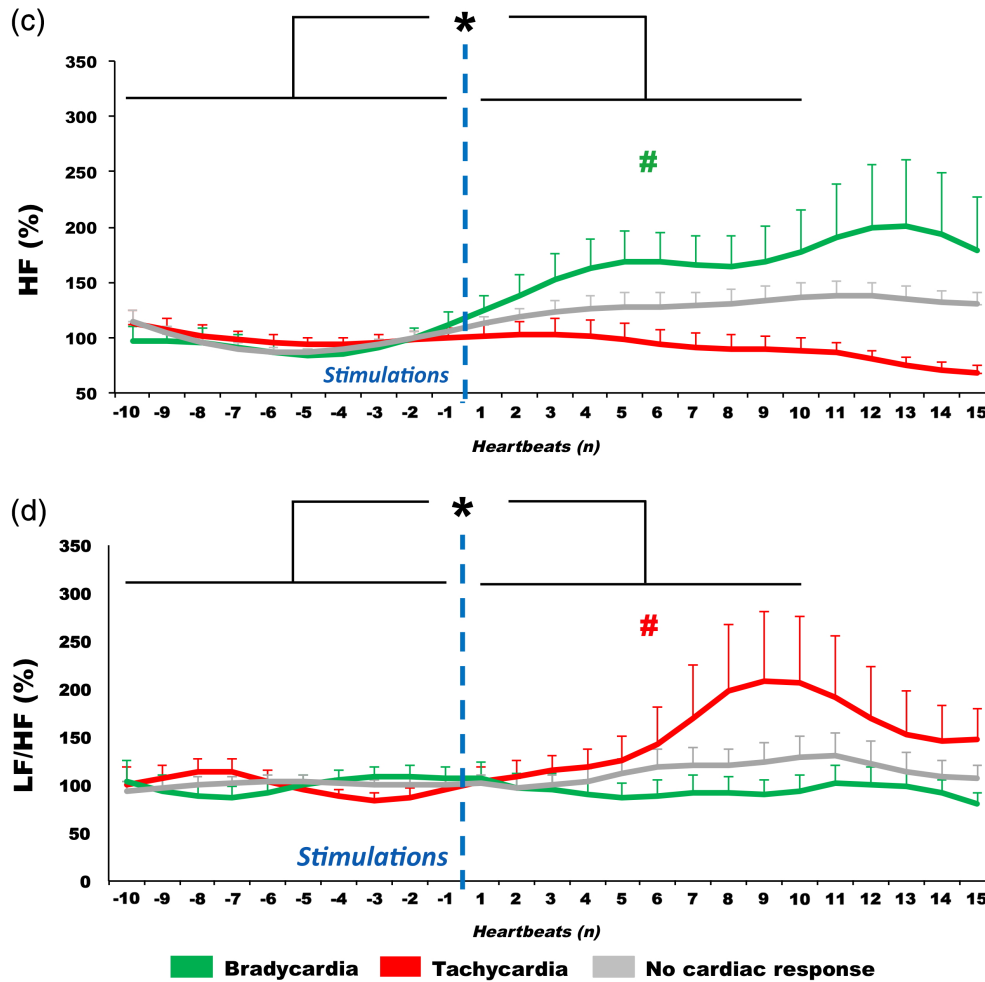


FIGURE 1 (Continued)

Very few studies have investigated the effects of cortical stimulation on heartbeat frequency in humans. They were carried out during brain surgery and examined the cingulate gyrus, temporal lobe, and orbitofrontal cortex (Chapman, Livingston, & Livingston, 1949; Delgado, 1960; Pool & Ransohoff, 1949; Smithwick & Chapman, 1949). Both pressor and depressor responses in blood pressure were elicited, but in only one study changes in RRI were recorded (Pool &

Ransohoff, 1949). Changes in RRI have already been elicited by stimulation of rat posterior insula (Marins et al., 2016; Oppenheimer & Cechetto, 1990) and primate anteroventral insula (Hoffman & Rasmussen, 1953; Kaada, 1951). However, in humans, Penfield and Faulk (1955) did not produce any cardiac effects by insular stimulation, and other studies focusing on insula stimulations (Penfield & Faulk, 1955; Mazzola, Mauguière, & Isnard, 2017 for a review) did not address this question. To our knowledge, the only previous study questioning cardiac effects of insular cortex stimulation in humans is that by Oppenheimer et al. (1992). In this study insular stimulations were conducted in patients during epilepsy surgery; three patients were stimulated in the right insula, and the two others, in the left insula. Of 70 stimulations, 50% resulted in changes in either RRI alone or accompanied by changes in blood pressure, demonstrating for the first-time cardiovascular changes after direct insular stimulation. This percentage of RRI changes is very similar to that of our study.

**TABLE 2** Talairach coordinates. Mean  $\pm$  SD according to cardiac evoked responses. Tachycardia, bradycardia, and no cardiac responses, and according to left and right insula stimulation side

	Talairach coordinates		
	x	y	z
Tachycardia	36.2 $\pm$ 3.3	-13.1 $\pm$ 9.8	9.8 $\pm$ 8
Left	35.0 $\pm$ 2.8	-9.8 $\pm$ 9.2	13.5 $\pm$ 5.6
Right	37.0 $\pm$ 3.7	-15.2 $\pm$ 10.4	5.8 $\pm$ 8.5
Bradycardia	36.7 $\pm$ 3.6	-6.7 $\pm$ 8.6	7.4 $\pm$ 9.4
Left	36.9 $\pm$ 3.4	-4.6 $\pm$ 7.8	5.5 $\pm$ 8.9
Right	36.1 $\pm$ 4.1	-10.8 $\pm$ 9.2	11.2 $\pm$ 9.7
No cardiac response	37.5 $\pm$ 3.8	-5.3 $\pm$ 10.8	7.3 $\pm$ 7.7
Left	36.8 $\pm$ 3.7	-6.7 $\pm$ 12.4	7.2 $\pm$ 7.6
Right	38.0 $\pm$ 3.9	-4.3 $\pm$ 9.4	7.4 $\pm$ 8

Oppenheimer et al. (1992) reported that more changes in RRI were elicited from the anterior than from the posterior right insular cortex; whereas on the left side, significantly more changes in RRI were generated from the posterior than from the anterior regions. In their study, bradycardia was observed more frequently after stimulations of the left insular cortex; whereas tachycardia was more often



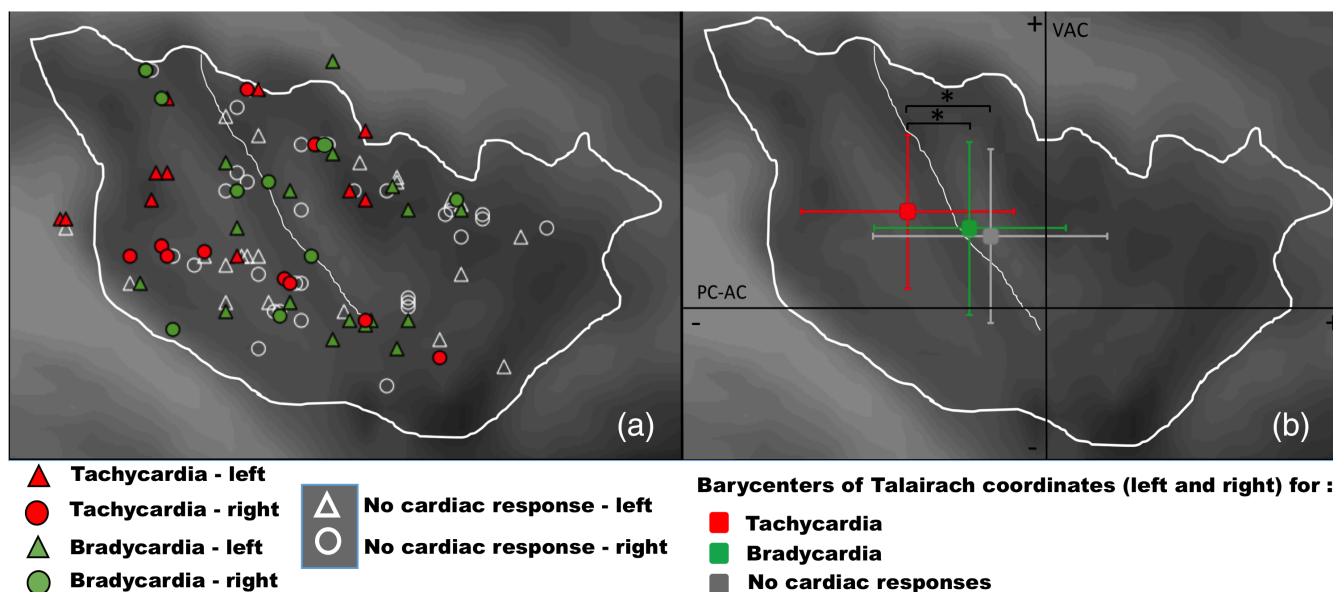


**FIGURE 2** Spatial distribution of evoked cardiac responses according to (a) their Talairach coordinates; (b) the barycenters and standard deviations of their Talairach coordinates (y and z axes). Despite an overlap in the location of the different type of cardiac responses, the location of stimulation sites evoking tachycardia were more posterior than those evoking bradycardia or no cardiac response (y-axis,  $p = 0.013$ ). Due to interindividual variability of insula anatomy, some contacts are located outside this virtual line, although located in the insula individually, for each patient. Some stimulation sites could not be illustrated by circles, either because their coordinates were identical in several patients or because they were located at different contact depths along the x-axis of the same electrode. For illustration, a sagittal insular mean image averaged from 24 subjects was superimposed onto the spatial distribution of stimulation site stereotactic coordinates. PC-AC: posterior commissure-anterior commissure horizontal plane; VAC: vertical anterior commissure coronal plane. \* $p < 0.05$

elicited after stimulation of the right insular cortex. These data were obtained in five patients, and by stimulating the ventral part of the insula after resection of the superior temporal gyrus, leaving unexplored a large part of the insular cortex in four of the five patients. If we consider stimulations that we performed in the ventral part of insula, we can explain why Oppenheimer et al. (1992) found this lateralization of responses, with tachycardiac responses being more represented on the right side and bradycardiac responses more represented on the left side in this part of the insular cortex.

The changes in RRI that we induced by insula stimulations were subtle, comparable to those reported by Oppenheimer et al. (1992) with means of six beats per minute for tachycardia and five beats per minute for bradycardia, explaining why insular stimulation studies (Mazzola, Mauguière, & Isnard, 2017; Pugnaghi et al., 2011; Stephani, Fernandez-Baca Vaca, Maciunas, Koubeissi, & Lüders, 2011) that did not address specifically this question did not report this finding. The bipolar type and the low intensity of our stimulation paradigm ensure a good spatial specificity of stimulations but may also explain the smallness and brevity of induced changes in heart rate. The timing of cardiac responses evoked is also consistent with what is known of the physiology of the ANS (Akselrod et al., 1981; Pomeranz et al., 1985). The sympathetic effects are slow, on a time scale between 6 and 25 s, corresponding to LF power of RR variability (0.04–0.15 Hz); whereas the parasympathetic effects are fast, on a time scale between 2 and 6 s, corresponding to HF power (0.15–0.40 Hz). This time scale difference between sympathetic and parasympathetic control is consistent with the fact that bradycardia occurred faster than tachycardia after insula stimulation (see Figure 1a). The time delay between the maximal variations of the RRI and those of the LF/HF ratio is explained by

the fact that the LF/HF ratio partly reflects slow oscillations (between 6 and 25 s); thus consistent with a maximum response reached at 9 s after the start of stimulation, while variations of RRI are faster (Pichot et al., 1999; Tanaka & Hargens, 2004). In the case of tachycardia, although the LF is not modified, the absence of modification in HF and the increase in the LF/HF ratio let us suppose that it is indeed a sympathetic activation which is underlying tachycardia. This is related to the nonspecificity of the LF that is under both sympathetic and parasympathetic controls (Malliani et al., 1991). Lastly, the absence of correlation between the cardiac response and the type of clinical symptoms evoked by stimulation strengthens the direct role of the insular cortex in autonomic control. It will be useful to compare the cardiac effects we report here with those that might be produced by stimulating other cortical regions involved in autonomic control. Further studies are needed to better understand how the structures of the central autonomic network are organized in the control of the cardiovascular system.

Several neuroimaging studies investigating brain activation patterns associated with cardiovascular responses are available (Beissner et al., 2013; Gray, Rylander, Harrison, Wallin, & Critchley, 2009; Napadow et al., 2008; Ruiz Vargas et al., 2016). However, small sample sizes, differences in methodologies and activation paradigms often associated with the generation of bodily arousal responses under cognitive, affective, and physiologic stress complicate the interpretation of the results. Two recent meta-analyses of functional imaging studies suggested that the insula is part of the central autonomic network (Beissner et al., 2013; Ruiz Vargas et al., 2016), but the exact location of cardiac representation in the insular cortex and its lateralization are still a matter of debate. Some studies suggested the possibility of a

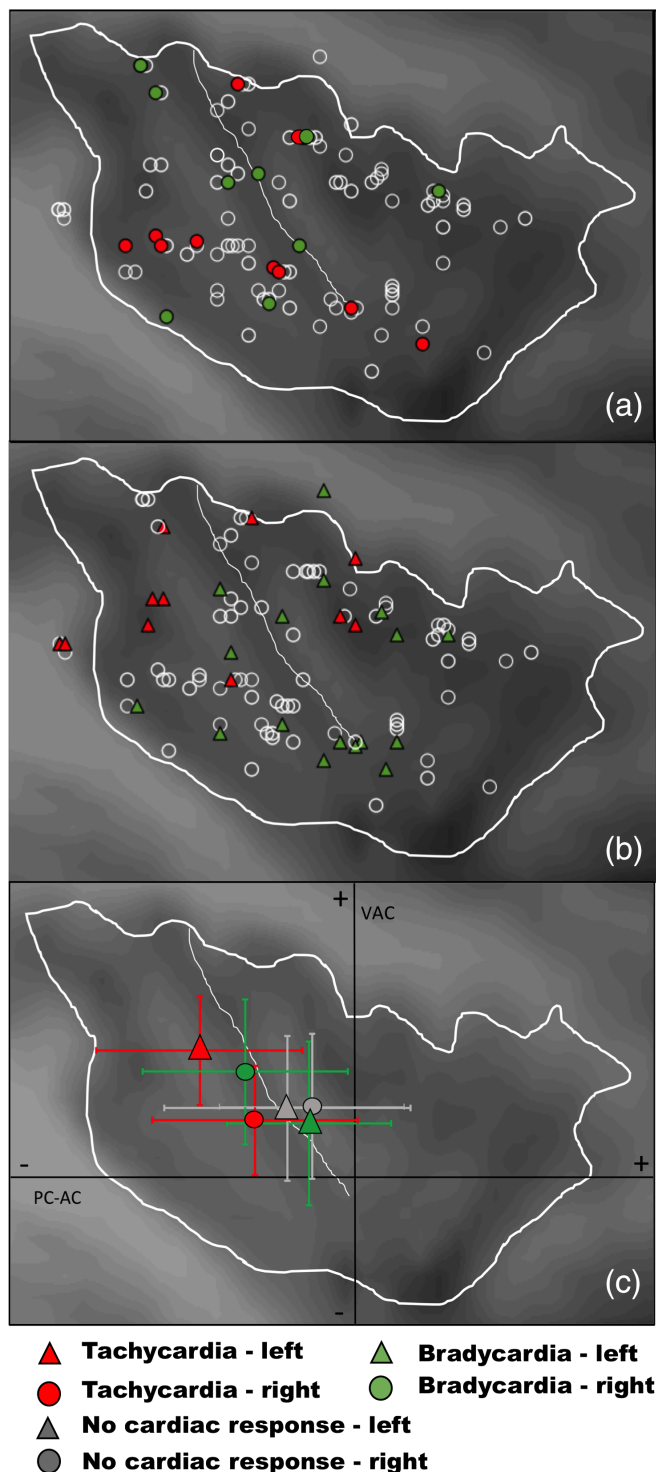


**FIGURE 3** Spatial distribution of evoked cardiac responses according to the stimulation side, in right (a) and left insula (b). The barycenters and standard deviations of their Talairach coordinates (y and z axes) in right (c) and left (d). Insula show that although left and right stimulations induced as much tachycardia as bradycardia, the implication of different insular subregions depended on the side stimulated: Tachycardia was preferentially evoked by stimulating insula in its right ventral posterior part, and in its left dorsal posteromedian part, whereas bradycardia was mainly induced by stimulations in the right dorsal insula and in the left ventral insula. PC-AC: posterior commissure-anterior commissure horizontal plane; VAC: vertical anterior commissure coronal plane [Color figure can be viewed at [wileyonlinelibrary.com](http://wileyonlinelibrary.com)]

lateralization of insular cortex in terms of cardiac function, with the right insula being more involved in sympathetic regulation and the left one in parasympathetic cardiac regulation (Oppenheimer & Cechetto, 2016; Ruiz Vargas et al., 2016, for a review). On the contrary, others did not conclude on any lateralization (Beissner et al., 2013). In the same way, the anteroposterior distribution of activations or deactivations evidenced by functional neuroimaging studies varies across studies. Here, based on responses to direct electrical stimulation, we observed that the insular representation of tachycardia is more posterior than that of bradycardia and that both types of cardiac responses are equally represented in right and left insula, in agreement with electrical stimulations in animals (Marins et al., 2016; Oppenheimer & Cechetto, 1990). This is also consistent with the insular descending pathways projecting on the subcortical regions described, including the nucleus ambiguus, dorsale motor nucleus and the rostroventral medulla, through the periaqueductal gray, parabrachial nuclei, nucleus tractus solitarius, and hypothalamus (Cechetto & Chen, 1990; Hyam, Kringelbach, Silburn, Aziz, & Green, 2012; Salman, 2016; Saper, 1982; Shivkumar et al., 2016).

One limitation in these neuroimaging studies is that cardiac activation paradigms, including physical, emotional, and cognitive tasks, give rise to a combination of effects that are difficult to dissociate from cardiovascular activation itself. This also raises the question whether the observed responses are top down (i.e., originating in the insula) or bottom up (i.e., insular response to peripheral heart input). Direct electrical stimulation of the insula in conscious patients, which bypasses these interferences, enables one to infer a causal relationship between the evoked modification of heart rate and the insular control of sympathetic and parasympathetic tones.

Our study suffers from two limitations: neither blood pressure nor respiration was monitored. During 70 intraoperative insular stimulations conducted under fentanyl neuroleptanesthesia in their five patients, Oppenheimer et al. (1992) reported that tachycardia responses accompanied by a decrease in blood pressure, or bradycardia response accompanied by an increase in blood pressure, were seen in 36% of stimulations that produced heart rate effects associated with blood pressure changes. However, the possibility that some of the cardiac responses we observed could be secondary to blood pressure changes via a reflex activation of peripheral baroreceptors looks unlikely. Cardiac responses were present from the onset of stimulation and remained stable during the entire stimulation. If stimulation had caused changes in blood pressure, the activation of the peripheral baroreceptors would have been fully expressed only after several seconds, so later than the heart rate changes that we have recorded (Shivkumar et al., 2016). Another argument comes from RRI variability analysis that reinforces our interpretation that tachycardia was due to an increased sympathetic tone and not to a decreased parasympathetic tone in response to a decrease in blood pressure. Similarly, bradycardia was due to an increased parasympathetic tone and not to a decrease in sympathetic tone triggered by an increase in blood pressure. Changes in respiratory activity are able to modify cardiac autonomic activity, particularly parasympathetic activity (Machado, 2013), as in the case of sleep apnea (Chouchou, Pichot, Barthélémy, Bastuji, & Roche, 2014). To our knowledge, no respiratory change has ever been reported in response to insular stimulations. Oppenheimer et al. (1992)

monitored respiration in one patient during insula stimulations and did not report any change. Nobis et al. (2018) have shown that electrical stimulation of the amygdala can lead to apneas but with stimulations of longer durations (between 5 and 30 s) and at higher intensities (at least 4 mA) than those used in our study (3–5 s) with an average intensity at 1.6 mA (Nobis et al., 2018). It remains that our results, obtained in a clinical setting that was not designed to study specifically the cardiovascular and respiratory systems, deserve further investigations including blood pressure and respiration rate monitoring for a more complete physiological interpretation of cardiac responses.

In human epilepsy, there is a strong association between tachycardia (Eggleston, Olin, & Fisher, 2014; Kato et al., 2014; Opherk & Hirsch, 2002) or cardiac asystole (Britton, Ghearing, Benarroch, & Cascino, 2006; Rocamora, Kurthen, Lickfett, Von Oertzen, & Elger, 2003; Schuele et al., 2007) and temporal lobe seizures. Chouchou et al. (2017) recently reported in a SEEG study of temporal lobe seizures the pivotal role of hippocampus and amygdala in ictal tachycardia, which can occur independently of insular ictal activity. Conversely, even if data are scarce, several observations suggest that insular seizures may lead to potentially life threatening autonomic disturbances, such as bradycardia (Britton et al., 2006; Rocamora et al., 2003; Schuele et al., 2007; Seeck et al., 2003), atrioventricular block (Surges, Scott, & Walker, 2009), and asystole (Seeck et al., 2003; Surges et al., 2009; Tayah, Savard, Desbiens, & Nguyen, 2013). To our knowledge, there is only one report in the literature of a single patient in whom an insular seizure with ictal asystole was recorded with multiple electrodes implanted in the left insula (Catenox, Mauguère, Guénot, Isnard, & Ryvlin, 2013). In this patient the electrode implanted in the posterior long gyrus showed a high frequency discharge starting 2 s before asystole. Our results support the possibility of a proper role of the insula in some dysautonomic seizures. They strengthen the need to explore the insula during presurgical evaluation of refractory epilepsy, when tachycardia or bradycardia are at the forefront, especially when heart rate changes are associated with other ictal symptoms evoking an insular origin of seizures (Isnard, Guénot, Sindou, & Mauguère, 2004; Obaid, Zerouali, & Nguyen, 2017). Our findings also show that low intensity electrical stimulation of the insula in preoperative exploration of perisylvian epilepsies can be considered as safe, knowing the brevity and subtleness of induced heart rate changes.

In addition, our work reinforces some studies showing functional and structural alterations of the insula in cardiovascular diseases such as hypertension (Marins, Iddings, Fontes, & Filosa, 2017) or heart failure (Song, Roy, Fonarow, Woo, & Kumar, 2018). These insula alterations would maintain sympathetic hyperactivity and parasympathetic dysfunction, while it is well documented that these autonomic alterations predict morbidity and mortality in these populations (Malliani et al., 1991). In particular, a neurovascular remodeling of the insular cortex was revealed in hypertension, which may contribute to the maintenance of sympathetic hyperactivity and of hypertension (Marins et al., 2017). In heart failure, Song et al. (2018) reported functional and structural alterations in the insula correlated with autonomic dysfunctions. Lastly, insular strokes have been associated with increased mortality (Laredo et al., 2018). Consistent with the present work, these studies converge to demonstrate an important role of the insula in autonomic dysfunctions in cardiovascular diseases.

Finally, Oppenheimer and Cechetto (2016) recently proposed that sensory perceptions could be imbued with autonomic color in the insula, which thus contributes to their emotional salience. It is noteworthy that the representation of cardiac control in the insula largely overlaps those of somatosensory visceral and vestibular responses as assessed by direct stimulations (see Mazzola, Royet, et al., 2017 for a review); this supports the view that cardiac responses could signify more than a mere involvement of the insula in physiological homeostasis.

## 5 | CONCLUSION

These findings indicate a posterior predominance of the sympathetic control in the insula, whatever the side, whereas the parasympathetic control seems more anterior. Dysfunction of these regions should be considered when modifications of cardiac activity occur during epileptic seizures.

## CONFLICT OF INTERESTS

The authors declare no conflict of interest.

## ORCID

Florian Chouchou  <https://orcid.org/0000-0003-0150-8159>

## REFERENCES

- Akselrod, S., Gordon, D., Ubel, F. A., Shannon, D. C., Berger, A. C., & Cohen, R. J. (1981). Power spectrum analysis of heart rate fluctuation: A quantitative probe of beat-to-beat cardiovascular control. *Science*, *213*, 220–222.
- Beissner, F., Meissner, K., Bär, K.-J., & Napadow, V. (2013). The autonomic brain: An activation likelihood estimation meta-analysis for central processing of autonomic function. *Journal of Neuroscience: The Official Journal of the Society for Neuroscience*, *33*, 10503–10511.
- Benarroch, E. E. (1993). The central autonomic network: Functional organization, dysfunction, and perspective. *Mayo Clinic Proceedings*, *68*, 988–1001.
- Britton, J. W., Ghearing, G. R., Benarroch, E. E., & Cascino, G. D. (2006). The ictal bradycardia syndrome: Localization and lateralization. *Epilepsia*, *47*, 737–744.
- Catenox, H., Mauguère, F., Guénot, M., Isnard, J., & Ryvlin, P. (2013). Recording the insula during ictal asystole. *International Journal of Cardiology*, *169*, e28–e30.
- Cechetto, D. F. (2014). Cortical control of the autonomic nervous system. *Experimental Physiology*, *99*, 326–331.
- Cechetto, D. F., & Chen, S. J. (1990). Subcortical sites mediating sympathetic responses from insular cortex in rats. *The American Journal of Physiology*, *258*, R245–R255.
- Chapman, W. P., Livingston, R. B., & Livingston, K. E. (1949). Frontal lobotomy and electrical stimulation of orbital surface of frontal lobes; Effect on respiration and on blood pressure in man. *Archives of Neurology and Psychiatry*, *62*, 701–716.
- Chouchou, F., Bouet, R., Pichot, V., Catenox, H., Mauguère, F., & Jung, J. (2017). The neural bases of ictal tachycardia in temporal lobe seizures. *Clinical Neurophysiology*, *128*, 1810–1819.
- Chouchou, F., & Dessesilles, M. (2014). Heart rate variability: A tool to explore the sleeping brain? *Frontiers in Neuroscience*, *8*, 402.
- Chouchou, F., Pichot, V., Barthélémy, J.-C., Bastuji, H., & Roche, F. (2014). Cardiac sympathetic modulation in response to apneas/hypopneas through heart rate variability analysis. Ed. Andrea Barbuti. *PLoS One*, *9*, e86434.

- Chouchou, F., Pichot, V., Perchet, C., Legrain, V., Garcia-Larrea, L., Roche, F., & Bastuji, H. (2011). Autonomic pain responses during sleep: A study of heart rate variability. *European Journal of Pain (London, England)*, *15*, 554–560.
- Critchley, H. D. (2005). Neural mechanisms of autonomic, affective, and cognitive integration. *The Journal of Comparative Neurology*, *493*, 154–166.
- Critchley, H. D., & Harrison, N. A. (2013). Visceral influences on brain and behavior. *Neuron*, *77*, 624–638.
- Daskalov, I., & Christov, I. (1997). Improvement of resolution in measurement of electrocardiogram RR intervals by interpolation. *Medical Engineering & Physics*, *19*, 375–379.
- Delgado, J. M. (1960). Circulatory effects of cortical stimulation. *Physiological Reviews. Supplement*, *4*, 146–178.
- Eggleston, K. S., Olin, B. D., & Fisher, R. S. (2014). Ictal tachycardia: The head-heart connection. *Seizure*, *23*, 496–505.
- Gray, M. A., Rylander, K., Harrison, N. A., Wallin, B. G., & Critchley, H. D. (2009). Following one's heart: Cardiac rhythms gate central initiation of sympathetic reflexes. *Journal of Neuroscience: The Official Journal of the Society for Neuroscience*, *29*, 1817–1825.
- Guyenet, P. G. (2006). The sympathetic control of blood pressure. *Nature Reviews. Neuroscience*, *7*, 335–346.
- Hoffman, B. L., & Rasmussen, T. (1953). Stimulation studies of insular cortex of *Macaca mulatta*. *Journal of Neurophysiology*, *16*, 343–351.
- Hyam, J. A., Kringelbach, M. L., Silburn, P. A., Aziz, T. Z., & Green, A. L. (2012). The autonomic effects of deep brain stimulation—a therapeutic opportunity. *Nature Reviews. Neurology*, *8*, 391–400.
- Isnard, J., Guénot, M., Sindou, M., & Mauguière, F. (2004). Clinical manifestations of insular lobe seizures: A stereo-electroencephalographic study. *Epilepsia*, *45*, 1079–1090.
- Kaada, B. R. (1951). Somato-motor, autonomic and electrocorticographic responses to electrical stimulation of rhinencephalic and other structures in primates, cat, and dog: A study of responses from the limbic, subcallosal, orbito-insular, piriform and temporal cortex, hippocampus-fornix and amygdala. *Acta Physiologica Scandinavica. Supplementum*, *24*, 1–262.
- Kato, K., Jin, K., Itabashi, H., Iwasaki, M., Kakisaka, Y., Aoki, M., & Nakasato, N. (2014). Earlier tachycardia onset in right than left mesial temporal lobe seizures. *Neurology*, *83*, 1332–1336.
- Kurth, F., Zilles, K., Fox, P. T., Laird, A. R., & Eickhoff, S. B. (2010). A link between the systems: Functional differentiation and integration within the human insula revealed by meta-analysis. *Brain Structure & Function*, *214*, 519–534.
- Lacuey, N., Hampson, J. P., Theeranaew, W., Zonjy, B., Vithala, A., Hupp, N. J., ... Lhatoo, S. D. (2017). Cortical structures associated with human blood pressure control. *JAMA Neurology*, *75*, 194–202.
- Laredo, C., Zhao, Y., Rudilosso, S., Renú, A., Pariente, J. C., Chamorro, Á., & Urra, X. (2018). Prognostic significance of infarct size and location: The case of insular stroke. *Scientific Reports*, *8*, 9498.
- Machado, B. H. (2013). Central control of autonomic and respiratory functions in health and diseases. *Autonomic Neuroscience: Basic & Clinical*, *175*, 1–2.
- Malliani, A., Pagani, M., Lombardi, F., & Cerutti, S. (1991). Cardiovascular neural regulation explored in the frequency domain. *Circulation*, *84*, 482–492.
- Marins, F. R., Iddings, J. A., Fontes, M. A. P., & Filosa, J. A. (2017). Evidence that remodeling of insular cortex neurovascular unit contributes to hypertension-related sympathoexcitation. *Physiological Reports*, *5*, e13156.
- Marins, F. R., Limborço-Filho, M., Xavier, C. H., Biancardi, V. C., Vaz, G. C., Stern, J. E., ... Fontes, M. A. P. (2016). Functional topography of cardiovascular regulation along the rostrocaudal axis of the rat posterior insular cortex. *Clinical and Experimental Pharmacology & Physiology*, *43*, 484–493.
- Mazzola, L., Isnard, J., & Mauguière, F. (2006). Somatosensory and pain responses to stimulation of the second somatosensory area (SII) in humans. A comparison with SI and insular responses. *Cerebral Cortex*, *16*, 960–968.
- Mazzola, L., Lopez, C., Faillenot, I., Chouchou, F., Mauguière, F., & Isnard, J. (2014). Vestibular responses to direct stimulation of the human insular cortex: Insula stimulation response. *Annals of Neurology*, *76*, 609–619.
- Mazzola, L., Mauguière, F., & Isnard, J. (2017). Electrical stimulations of the human insula: Their contribution to the ictal semiology of insular seizures. *Journal of Clinical Neurophysiology*, *34*, 307–314.
- Mazzola, L., Royet, J.-P., Catenoix, H., Montavont, A., Isnard, J., & Mauguière, F. (2017). Gustatory and olfactory responses to stimulation of the human insula. *Annals of Neurology*, *82*, 360–370.
- Napadow, V., Dhond, R., Conti, G., Makris, N., Brown, E. N., & Barbieri, R. (2008). Brain correlates of autonomic modulation: Combining heart rate variability with fMRI. *NeuroImage*, *42*, 169–177.
- Nathan, S. S., Sinha, S. R., Gordon, B., Lesser, R. P., & Thakor, N. V. (1993). Determination of current density distributions generated by electrical stimulation of the human cerebral cortex. *Electroencephalography and Clinical Neurophysiology*, *86*, 183–192.
- Nobis, W. P., Schuele, S., Templer, J. W., Zhou, G., Lane, G., Rosenow, J. M., & Zelano, C. (2018). Amygdala-stimulation-induced apnea is attention and nasal-breathing dependent. *Annals of Neurology*, *83*, 460–471.
- Obaid, S., Zerouali, Y., & Nguyen, D. K. (2017). Insular epilepsy: Semiology and noninvasive investigations. *J Clin Neurophysiol off Publ Am Electroencephalogr Soc*, *34*, 315–323.
- Opherk, C., & Hirsch, L. J. (2002). Ictal heart rate differentiates epileptic from non-epileptic seizures. *Neurology*, *58*, 636–638.
- Oppenheimer, S., & Cechetto, D. (2016). The insular cortex and the regulation of cardiac function. *Comprehensive Physiology*, *6*, 1081–1133.
- Oppenheimer, S. M., & Cechetto, D. F. (1990). Cardiac chronotropic organization of the rat insular cortex. *Brain Research*, *533*, 66–72.
- Oppenheimer, S. M., Gelb, A., Girvin, J. P., & Hachinski, V. C. (1992). Cardiovascular effects of human insular cortex stimulation. *Neurology*, *42*, 1727–1732.
- Pagani, M., Montano, N., Porta, A., Malliani, A., Abboud, F. M., Birkett, C., & Somers, V. K. (1997). Relationship between spectral components of cardiovascular variabilities and direct measures of muscle sympathetic nerve activity in humans. *Circulation*, *95*, 1441–1448.
- Penfield, W., & Faulk, M. E. (1955). The insula; Further observations on its function. *Brain: A Journal of Neurology*, *78*, 445–470.
- Pichot, V., Gaspoz, J. M., Molliex, S., Antoniadis, A., Busso, T., Roche, F., ... Barthélémy, J. C. (1999). Wavelet transform to quantify heart rate variability and to assess its instantaneous changes. *Journal of Applied Physiology (Bethesda, Md. : 1985)* *1985*, *86*, 1081–1091.
- Pichot, V., Roche, F., Celle, S., Barthélémy, J.-C., & Chouchou, F. (2016). HRVanalysis: A free software for analyzing cardiac autonomic activity. *Frontiers in Physiology*, *7*, 557. <http://journal.frontiersin.org/article/10.3389/fphys.2016.00557/abstract>
- Pomeranz, B., Macaulay, R. J., Caudill, M. A., Kutz, I., Adam, D., Gordon, D., ... Cohen, R. J. (1985). Assessment of autonomic function in humans by heart rate spectral analysis. *The American Journal of Physiology*, *248*, H151–H153.
- Pool, J. L., & Ransohoff, J. (1949). Autonomic effects on stimulating rostral portion of cingulate gyri in man. *Journal of Neurophysiology*, *12*, 385–392.
- Pugnaghi, M., Meletti, S., Castana, L., Francione, S., Nobili, L., Mai, R., & Tassi, L. (2011). Features of somatosensory manifestations induced by intracranial electrical stimulations of the human insula. *Clin Neurophysiol off J Int Fed Clin Neurophysiol*, *122*, 2049–2058.
- Rajendra Acharya, U., Paul Joseph, K., Kannathal, N., Lim, C. M., & Suri, J. S. (2006). Heart rate variability: A review. *Medical & Biological Engineering & Computing*, *44*, 1031–1051.
- Rocamora, R., Kurthen, M., Lickfett, L., Von Oertzen, J., & Elger, C. E. (2003). Cardiac asystole in epilepsy: Clinical and neurophysiologic features. *Epilepsia*, *44*, 179–185.
- Ruiz Vargas, E., Sörös, P., Shoemaker, J. K., & Hachinski, V. (2016). Human cerebral circuitry related to cardiac control: A neuroimaging meta-analysis. *Annals of Neurology*, *79*, 709–716.
- Salman, I. M. (2016). Major autonomic Neuroregulatory pathways underlying short- and long-term control of cardiovascular function. *Current Hypertension Reports*, *18*, 18.
- Saper, C. B. (1982). Reciprocal parabrachial-cortical connections in the rat. *Brain Research*, *242*, 33–40.
- Schuele, S. U., Bermeo, A. C., Alexopoulos, A. V., Locatelli, E. R., Burgess, R. C., Dinner, D. S., & Foldvary-Schaefer, N. (2007). Video-electrographic and clinical features in patients with ictal asystole. *Neurology*, *69*, 434–441.



- Seeck, M., Zaim, S., Chaves-Vischer, V., Blanke, O., Maeder-Ingvar, M., Weissert, M., & Roulet, E. (2003). Ictal bradycardia in a young child with focal cortical dysplasia in the right insular cortex. *European Paediatric Neurology Society*, 7, 177–181.
- Shivkumar, K., Ajjola, O. A., Anand, I., Armour, J. A., Chen, P.-S., Esler, M., ... Zipes, D. P. (2016). Clinical neurocardiology defining the value of neuroscience-based cardiovascular therapeutics. *The Journal of Physiology*, 594, 3911–3954.
- Smith, R., Thayer, J. F., Khalsa, S. S., & Lane, R. D. (2017). The hierarchical basis of neurovisceral integration. *Neuroscience and Biobehavioral Reviews*, 75, 274–296.
- Smithwick, R. H., & Chapman, E. M. (1949). The human heart rate; Some observations and deductions based upon the effect of removing portions of the sympathetic nervous system in man. *Surgery*, 26, 727–744.
- Song, X., Roy, B., Fonarow, G. C., Woo, M. A., & Kumar, R. (2018). Brain structural changes associated with aberrant functional responses to the Valsalva maneuver in heart failure. *Journal of Neuroscience Research*, 96, 1610–1622.
- Sörös, P., & Hachinski, V. (2012). Cardiovascular and neurological causes of sudden death after ischaemic stroke. *Lancet Neurology*, 11, 179–188.
- Stephani, C., Fernandez-Baca Vaca, G., Maciunas, R., Koubeissi, M., & Lüders, H. O. (2011). Functional neuroanatomy of the insular lobe. *Brain Structure & Function*, 216, 137–149.
- Surges, R., Scott, C. A., & Walker, M. C. (2009). Peri-ictal atrioventricular conduction block in a patient with a lesion in the left insula: Case report and review of the literature. *Epilepsy and Behavior*, 16, 347–349.
- Szurhaj, W., Troussière, A.-C., Logier, R., Derambure, P., Tyvaert, L., Semah, F., ... De Jonckheere, J. (2015). Ictal changes in parasympathetic tone: Prediction of postictal oxygen desaturation. *Neurology*, 85, 1233–1239.
- Tanaka, K., & Hargens, A. R. (2004). Wavelet packet transform for R-R interval variability. *Medical Engineering & Physics*, 26, 313–319.
- Tayah, T., Savard, M., Desbiens, R., & Nguyen, D. K. (2013). Ictal bradycardia and asystole in an adult with a focal left insular lesion. *Clinical Neurology and Neurosurgery*, 115, 1885–1887.
- Tokgözüoğlu, S. L., Batur, M. K., Topçuoğlu, M. A., Saribas, O., Kes, S., & Oto, A. (1999). Effects of stroke localization on cardiac autonomic balance and sudden death. *Stroke*, 30, 1307–1311.
- Verberne, A. J., & Owens, N. C. (1998). Cortical modulation of the cardiovascular system. *Progress in Neurobiology*, 54, 149–168.

**How to cite this article:** Chouchou F, Mauguière F, Vallayer O, et al. How the insula speaks to the heart: Cardiac responses to insular stimulation in humans. *Hum Brain Mapp.* 2019;40:2611–2622. <https://doi.org/10.1002/hbm.24548>